

Electrochemically deposited nano polyaniline films as hole transporting layers in organic solar cells

Yu-Kai Han^{a,*}, Mei-Ying Chang^b, Ko-Shan Ho^a, Tar-Hwa Hsieh^a, Jeng-Liang Tsai^b,
Pei-Chen Huang^a

^a Department of Chemical and Materials Engineering, National Kaohsiung University of Applied Sciences, Kaohsiung 807, Taiwan, Republic of China

^b Department of Photonics, National Sun Yat-sen University, Kaohsiung 804, Taiwan, Republic of China

ARTICLE INFO

Article history:

Received 1 July 2013

Received in revised form

3 March 2014

Accepted 27 April 2014

Keywords:

Polyaniline

Buffer layer

Power conversion efficiency

Transporting layer

PEDOT:PSS primary doping

ABSTRACT

In this study, we prepared organic solar cells based on poly(3-hexylthiophene) (P3HT) and [6,6]-phenyl-C₆₁-butyric acid methyl ester (PCBM) with electrochemically deposited nano polyaniline (PANI) buffer layers (either PANI – 0.1 M or PANI – 0.3 M) as hole transporting layers and compared their performances with those of solar cells lacking the buffer layer (i.e., bare ITO) or featuring buffer layers of poly(3,4-ethylenedioxythiophene):polystyrenesulfonate (PEDOT:PSS) or PEDOT:PSS-covered PANI. The power conversion efficiency of the device featuring PANI/PEDOT:PSS as the buffer layer (2.76%) was greater than those of devices featuring bare ITO (0.75%) or the PANI – 0.1 M (1.33%), PANI – 0.3 M (1.78%), or PEDOT:PSS (2.30%) layers. We suspect that the increased conductivity of the PANI/PEDOT:PSS composite, caused by interactions between the PANI nitrogen atoms and the functional groups of PSS, led to additional doping of PANI. This primary doping effect by PSS toward PANI lowered the series resistance of the PANI/PEDOT:PSS buffer layer and, thereby, increased the photocurrent of the device. As a result, electrochemically deposited PANI buffer layers, with or without PEDOT:PSS, appear to be promising hole transporting layers for organic electronic devices that require different candidate materials (other than PEDOT:PSS conductors) and/or different processing conditions (other than spin-coating).

© 2014 Elsevier B.V. All rights reserved.

1. Introduction

Although poly(3,4-ethylenedioxythiophene):polystyrenesulfonate (PEDOT:PSS) is insoluble in organic solvents, it is often employed as a transparent hole-transporting material in organic cells because of its high conductivity, simple processing, and suitable work function [1]. The use of PEDOT:PSS has several limitations: it degrades under UV illumination, it introduces water into the devices' active layer, and it retains a degree of acidity that can damage indium tin oxide (ITO) at high temperatures, thereby affecting the long-term stability of its devices [2]. Therefore, several highly conductive materials, including carbon nanotubes (CNTs) [3], polyhexylthiophene [4], and polyaniline (PANI) [5–7], have been studied as possible replacements for PEDOT:PSS as the hole injection or transporting layer.

Doping PEDOT with PSS allows it to become soluble in aqueous media, thereby facilitating its deposition onto ITO surfaces through spin-coating—the most common method employed in the fabrication of organic devices. Even though spin-coating is an inexpensive, rapid,

and simple means of depositing liquid materials, it can waste a lot of material, making it less attractive for manufacturing processes.

Several methods for the deposition of hole transporting (e.g., PEDOT:PSS, polyaniline (PANI)) and active layers—including inkjet printing [8], spray deposition [9], roll-to-roll gravure printing [10], brush painting [11], and screen printing [12]—have been developed to enhance the manufacturing process with the goal of mass production of organic electronics. The presence of PANI-coated ITO electrodes can decrease the operating voltage, increase the electroluminescence quantum efficiency, and improved device reliability of organic light emitting diodes (OLED) because they can lower the hole-injection barrier between the anode and the hole-transporting emissive layer [13–21]. Notably, the performance of ITO/PANI-based devices can be similar to that of corresponding ITO/PEDOT:PSS-based devices [20–22].

Recently, electrochemical polymerization was reported as an alternative means of depositing conductive polymers onto ITO surfaces for organic device applications [23–25]. Zhou et al. [23] electrochemically deposited PEDOT:PSS onto an ITO surface during the formation of a device having the configuration ITO/PEDOT:PSS/ZnO:MDMO-PPV/Al and obtained a power conversion efficiency (η) of 0.33% under AM 1.5 illumination. Mello et al. [24] used

* Corresponding author.

E-mail address: ykhan@cc.kuas.edu.tw (Y.-K. Han).

electrochemical polymerization to deposit sulfonated PANI (SPANI) and then prepared a device having the structure TO/SPANI/poly(3-methylthiophene)/Al that exhibited a value of η of 0.8% under monochromatic irradiation ($\lambda=580$ nm; 0.8 W/m²). Qu et al. [25] electrodeposited PANI as the anode buffer layer (thickness: 120 nm) in the device structure ITO/PANI/MDMO-PPV:PCBM/ZnO/Al and obtained a power conversion efficiency of 0.65%.

Although electrochemically deposited PANI films are promising materials for use in organic optoelectronics, the effects of the morphologies of these films on the photovoltaic performance of poly(3-hexylthiophene) (P3HT)/[6,6]-phenyl-C₆₁-butyric acid methyl ester (PCBM)-based organic solar cells (OSCs) have seldom been reported. It is well established [25–26] that the surface morphology of a film of an organic material can help or hinder the transport of carriers across various interfaces. In a previous report [26], we demonstrated that a tube-like PANI nanomaterial increased the photovoltaic performance of P3HT:PCBM-based devices when it acted as a hole-transport layer (HTL) between PEDOT:PSS and P3HT:PCBM layers; in other words, the morphology of the hole-transporting material played a key role affecting the photovoltaic properties of that device.

In this study, we prepared OSCs featuring HTLs with various surface morphologies—bare ITO, ITO presenting an electrochemically deposited PANI thin film, and a PANI – 0.3 M thin film spin-coated with PEDOT:PSS—and compared their photovoltaic properties [open-circuit voltage (V_{oc}); series resistance (R_s); short-circuit current density (J_{sc}); η] with respect to their different surface morphologies.

2. Experimental

Aniline (ANI) was doubly distilled prior to use and stored at 5 °C. Electrochemical experiments are performed in a three-electrode cell; patterned ITO glass, a platinum wire, and Ag/AgCl

functioned as the working electrode, counter electrode, and reference electrode, respectively. Cyclic voltammetry (CV) was performed using an AUTO-LAB apparatus. The PANI – 0.1 M and PANI – 0.3 M films were obtained after electro-polymerization of aqueous solutions containing 0.1 and 0.3 M ANI monomer, respectively, and 1 M H₂SO₄, applying a sequential linear potential scan rate of 0.01 V/s between –0.2 and +0.9 V versus the Ag/AgCl electrode. The PANI/PEDOT:PSS film was obtained by spin-coating a PEDOT:PSS (AI 4083) solution onto the ITO/PANI – 0.3 M surface and then drying at 150 °C for 20 min. Field emission scanning electron microscopy (FE-SEM) images of water- or hexane-diluted dispersions dried on cover glasses were recorded using a Hitachi FE-2000 apparatus. The surface morphologies of the films were characterized using a Ben-Yuan CSPM4000 scanning probe microscope and an atomic force microscope operated in the tapping mode. The film thickness was measured using a Dektak 6M stylus profilometer. Optical spectra were recorded using a UV–vis spectrophotometer; the work functions of the films were measured using a Riken Keiki AC-2 surface analyzer photoelectron spectrometer. The current density–voltage (J – V) characteristics were measured using a Keithley 2400 source meter while illuminating the devices with white light (100 mW/cm²) from a halogen lamp. A single-crystalline silicon solar cell was used as a reference cell to confirm the stability of the light source; the mismatch factor was not taken into account.

3. Results and discussion

3.1. Surface morphologies of devices

Smooth surface morphologies are required for anodes used in organic optoelectronic devices because “spikes” can cause breakdown and/or shorting, thereby affecting the performance [27].

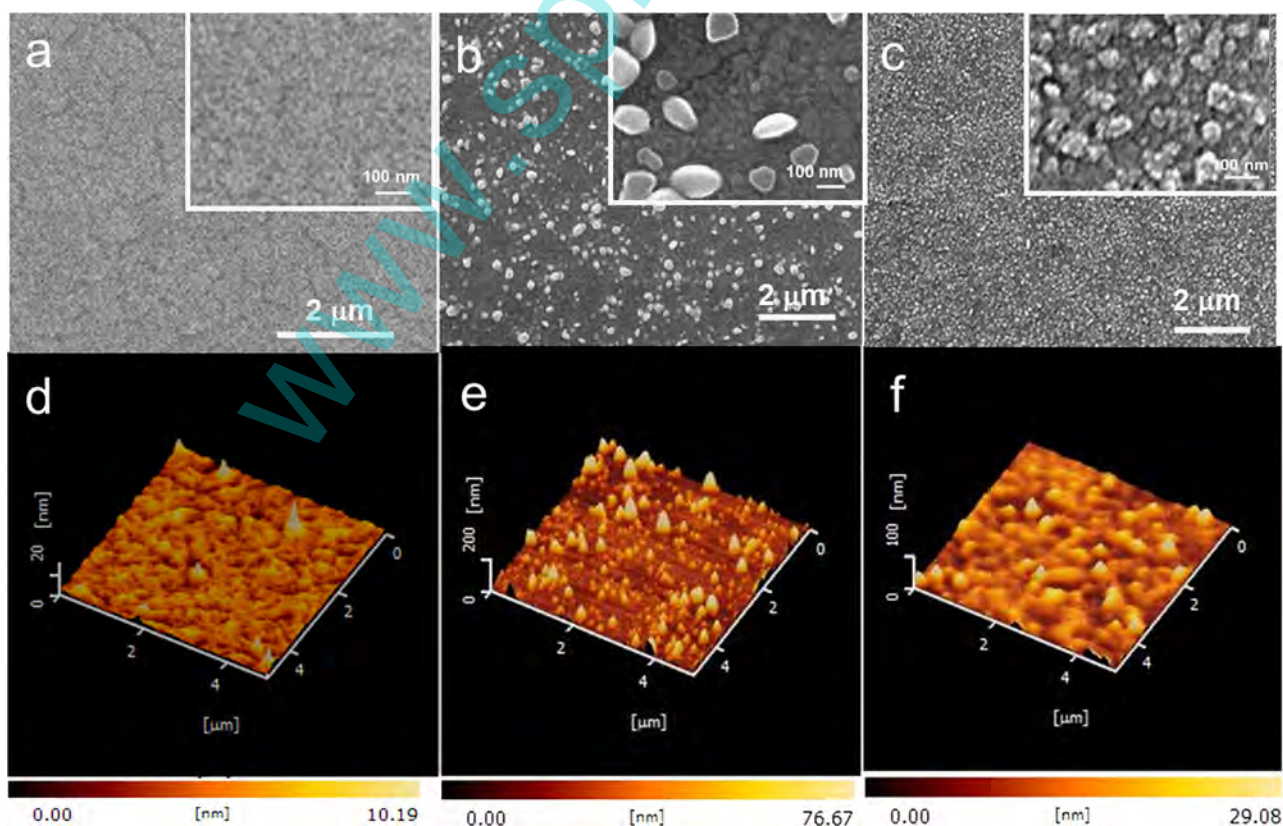


Fig. 1. (a)–(c) SEM and (d)–(f) AFM images of (a, d) ITO, (b, e) PANI – 0.1 M, and (c, f) PANI – 0.3 M films.

Fig. 1 displays the surface morphologies of the bare ITO and the ITO surfaces presenting PANI – 0.1 M and PANI – 0.3 M films as measured using scanning electron microscopy (SEM) and atomic force microscopy (AFM); Table 1 summarizes the surface roughnesses of these samples. The roughness of the bare ITO was in the range from 0 to 12 nm; it contained a few spikes that might result in shorting of the device—thereby affecting its photovoltaic performance—in the absence of a buffer layer. The nano PANI – 0.1 M particles grew discontinuously and were dispersed on the ITO surface; the roughness ranged between 9 and 94 nm. We obtained these PANI – 0.1 M particles by carefully adjusting the concentration of the ANI monomer and the electrochemical deposition potential, obtaining distinctive PANI nano films for use as HTLs. We obtained continuous nano PANI films after increasing the monomer concentration up to 0.3 M under otherwise identical electrochemical deposition parameters. The films of nano PANI – 0.3 M particles grown continuously and dispersed on the ITO surface had roughnesses between 5 and 35 nm. We suspected this continuous PANI nano film would effectively decrease the “spike” effect, relative to that obtained using the monomer concentration of 0.1 M, when deposited onto the ITO surface; accordingly, the lower roughness of this transporting layer surface would presumably lead to higher optoelectronic performance.

The root-mean-square (RMS) roughnesses of these PANI-modified ITO surfaces decreased upon increasing the PANI concentration; for example, the RMS roughness of PANI – 0.3 M (5.25 nm) was less than that of PANI – 0.1 M (9.76 nm). In addition, the RMS roughness of the PEDOT:PSS-covered ITO/PANI – 0.3 M film (ca. 3.10 nm) was less than those of the PANI – 0.1 M and PANI – 0.3 M films deposited on the ITO surfaces. The maximum roughness (R_{max}) of the PANI – 0.3 M film decreased from approximately 35 to 22 nm (Fig. 2) after its covering with a PEDOT:PSS layer and then drying of the sample at 150 °C for 20 min. This behavior reflects the marked tendency of PEDOT:PSS

layers to planarize ITO/PANI – 0.3 M surfaces, as summarized in Table 1 and Fig. 2.

3.2. Transmittance of buffer layers

Fig. 3 presents the transmittance spectra of the various samples tested in this study, as well as the UV–vis absorbance spectrum of the P3HT film, in the range 300–800 nm. To allow reasonable comparisons of the behavior of these films, we fixed the film thickness of each sample to within the range 40–60 nm, the same thickness of the layers used in the OSC devices.

The thickness of an HTL can affect the amount of incident light reaching a photoactive polymer. The transmittances of our PANI and PANI/PEDOT:PSS layers were greater than 80% in the wavelength range 450–800 nm, comparable with that of the PEDOT:PSS layer (> 88%); thus, the PANI film appeared suitable for use as the HTL layer in P3HT:PCBM-based OSC devices. In Fig. 3, the lower transmittance of the PANI-based films in the range 350–450 nm can be attributed to the π – π transitions of PANI. We observed no obvious differences in transmittance at 500–800 nm between the PANI and PEDOT:PSS films. The transmittance of the PANI/PEDOT:PSS film decreased slightly in the range 550–800 nm because the

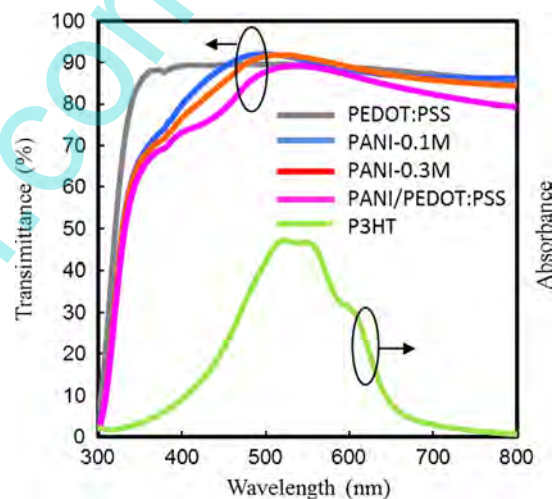


Fig. 3. Transmittance spectra of the samples used in this study (left-hand y-axis) and UV–vis absorbance spectrum of the P3HT film (right-hand y-axis), both in the range of 300–800 nm.

Table 1
Surface roughnesses of the samples used in this study.

Film	RMS (nm)	R_a (nm)	R_{max} (nm)
ITO	1.8	2.21	12
PANI – 0.1 M	9.79	6.03	94
PANI – 0.3 M	5.25	3.68	35
PANI/PEDOT:PSS	3.10	2.36	22

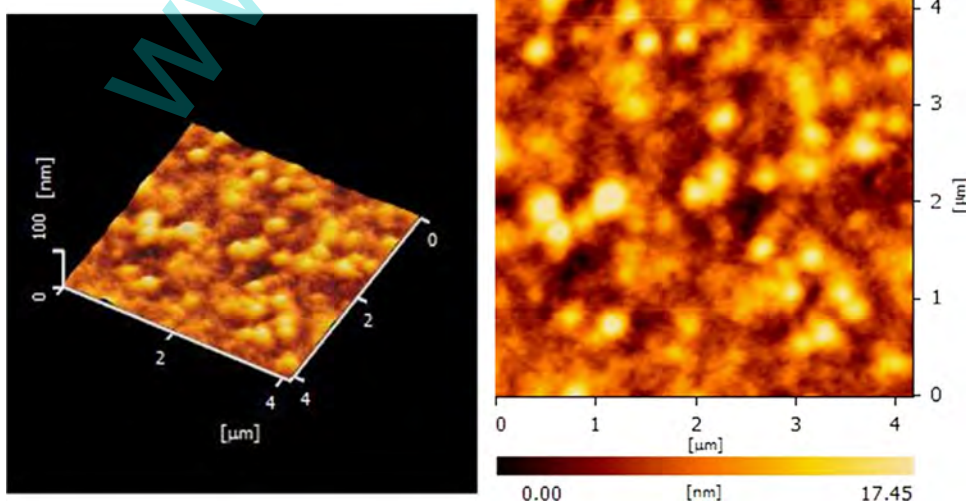
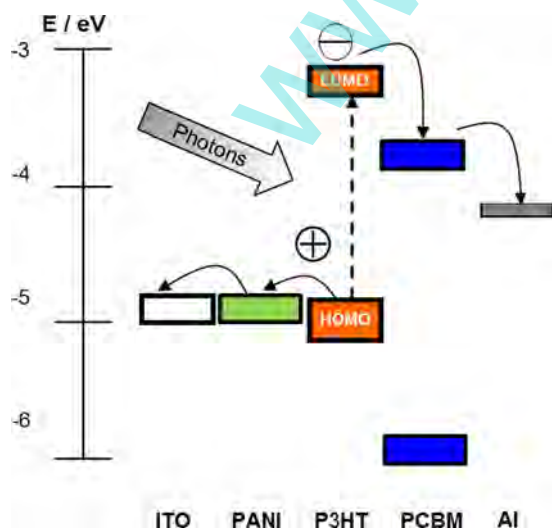


Fig. 2. AFM image of the ITO/PANI surface covered with PEDOT:PSS.

thickness of the PEDOT:PSS-covered PANI film was greater than that of the single PANI layer. Because the thickness of the electrochemically deposited PANI nano films can be tuned by varying the monomer concentration, these films are promising materials for use in applications that require high transparency.

The work function (ϕ_w) is the minimum energy required to remove an electron from the surface of a material; it is strongly affected by the morphology and/or surface reactions (e.g., oxidation) of a surface. Measuring the value of ϕ_w after electrochemical deposition of a PANI film can provide valuable information regarding the properties of a given film surface. The work function of PANI is approximately 4.8 eV, within the range of the values reported for plasma-treated ITO (4.5–5.11 eV) [28,29]. It has been demonstrated that ITO in combination with a *p*-doped transport layer provides a low voltage drop for hole injection. For this reason, we expected the similar work function of PANI to ensure efficient charge injection. The values of ϕ_w of our tested samples of ITO, PANI – 0.1 M, PANI – 0.3 M, and PANI/PEDOT:PSS were 4.8, 4.85, 4.9, and 4.9 eV, respectively. Because the PANI – 0.1 M film featured nano PANI particles that were not continuously distributed on the ITO surface, the value of ϕ_w was contributed in part by the individual values for ITO and PANI. In Fig. 1(c), PANI – 0.3 M appears as a continuous film on the ITO surface; accordingly, we obtained a higher value of ϕ_w of 4.9 eV. We attribute the relatively high value of ϕ_w of the PANI/PEDOT:PSS film (4.9 eV) to the presence of the covering PEDOT:PSS film, which decreases the roughness of the ITO/PANI surface and, thereby, decreased the chance of current leakage from the spikes on the PANI surface, leading to efficient electrical contact. Because the values of ϕ_w of these samples were all in the range of 4.8–4.9 eV, we can consider them to have similar minimum energies required to remove an electron from their surfaces, taking measurement errors into account. Thus, regardless of whether the surface was PANI or PEDOT:PSS, we suspected the nano PANI film would function as a good hole extracting and transporting layer in P3HT-based OSC devices.

Scheme 1 displays the energy levels of the compounds tested in this study. The active layer absorbed photons to form excitons that separated into free charge carriers at the *p*-*n* heterojunction interfaces under the internal electric field. The holes would pass through a well-defined contact surface between the interfaces; efficient pathways would allow transportation of the free charge carriers toward their respective electrodes, thereby decreasing the degree of exciton recombination within the photoactive cell.



Scheme 1. Energy levels of the compounds used in this study.

3.3. Performance of OSCs

We analyzed the photovoltaic characteristics of the devices based on the equivalent circuit; this approach has been used frequently to describe the electric behavior of photovoltaic devices [30]. The *J*-*V* characteristics can be described by the dark *I*-*V* curve and fitted by the standard one-diode model

$$I = I_0 \left[\exp\left(\frac{q(V - IR_S)}{nkT}\right) - 1 \right] + \frac{q(V - IR_S)}{R_{SH}} \quad (1)$$

where I_0 is the saturation current, q is the magnitude of the electronic charge, V is the applied voltage, n is the ideality factor, k is Boltzmann's constant, T is the absolute temperature, R_S is the series resistance, R_{SH} is the shunt resistance, and I_{PH} is the photocurrent. The series resistance can be estimated from the inverse slope at a positive voltage where the *I*-*V* curves become linear; a lower series resistance will result in a higher current flowing through a device. Fig. 4 presents the *J*-*V* curves of the P3HT:PCBM-based solar cells featuring various buffer layers under AM 1.5 solar illumination. Table 2 lists the values of R_S that we obtained from the *J*-*V* curves of the devices; a significant decrease in the value of R_S occurred when the device incorporated a buffer layer modified with the PANI – 0.3 M/PEDOT:PSS layer. The series resistance, which can be expressed as the sum of the bulk and interfacial resistances, can reflect the ohmic loss in solar cells; ohmic loss includes the resistances of the organic/electrode contacts, the photoactive layer, and the electrodes as well as the parasitic probe resistance [31]. We suspect that the three interfaces featuring the introduced PANIs (i.e., the ITO/PANI, PANI/PEDOT:PSS, and PEDOT:PSS/active layer interfaces) provided series

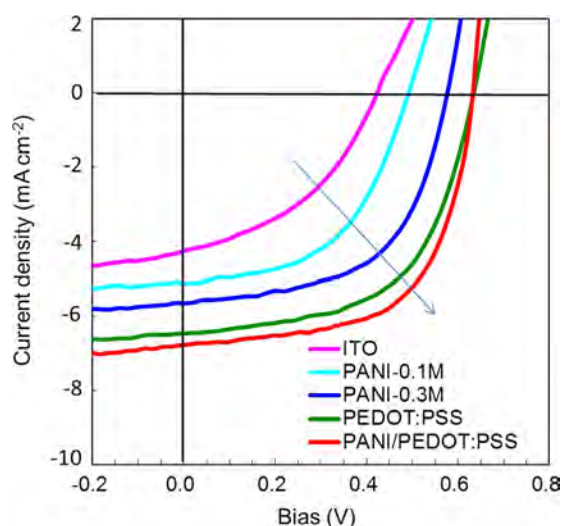
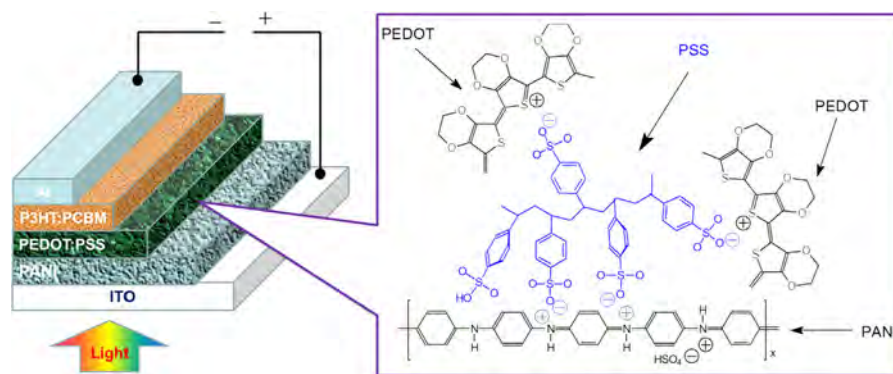


Fig. 4. Current-voltage characteristics (AM 1.5 G, 100 mW/cm²) of the devices prepared in this study.

Table 2
Characteristics of the photovoltaic cells measured under AM 1.5 G (100 mW/cm²) solar illumination.

Buffer layer ^a	J_{sc} (mA/cm ²)	V_{oc} (V)	FF (a.u.)	η (%)	R_S (Ω cm ²)
w/o Buffer layer	4.31	0.42	0.42	0.75	51.8
PANI – 0.1 M	5.11	0.51	0.51	1.33	41.5
PANI – 0.3 M	5.67	0.56	0.56	1.78	32.9
PEDOT:PSS	6.41	0.64	0.56	2.31	31.3
PANI – 0.3 M/PEDOT:PSS	7.03	0.64	0.61	2.76	25.1

^a Device structure: ITO/buffer layer/P3HT:PCBM/Al.



Scheme 2. Schematic representation of the primary doping effect between PSS and PANI.

resistances much lower in magnitude relative to that of the ITO/PEDOT:PSS/active layer contact.

For bulk heterojunction devices, the value of V_{OC} correlates directly with the energy difference between the highest occupied molecular orbital (HOMO) of the donor and the lowest unoccupied molecular orbital (LUMO) of the acceptor. For P3HT:PCBM-based devices, the energy difference between the HOMO and LUMO levels of P3HT and PCBM is 0.6 eV. The values of V_{OC} of the PANI – 0.1 M and bare ITO solar cell devices were lower than those of the devices featuring PEDOT:PSS or PANI – 0.3 M/PEDOT:PSS as the buffer layer. We suspect that a large concentration of holes aggregated at the anode because of poor interfacial contact (i.e., at the ITO/P3HT:PCBM interface) for the bare-ITO device and for the non-continuous nano PANI – 0.1 M layer containing partially good (i.e., ITO/PANI and PANI/P3HT:PCBM interfaces) and partially poor (i.e., ITO/P3HT) interfaces for carrier transport.

The P3HT:PCBM-based solar cell lacking the buffer layer (bare ITO) exhibited the lowest power conversion efficiency among our tested samples. Thus, the high injection barrier of ITO limited the transfer of holes to the anode and, thereby, minimized the current; this phenomenon can be improved by depositing a suitable HTL (e.g., PEDOT:PSS) through spin-coating [32–35].

In this study, we electrochemically deposited PANI – 0.1 M and PANI – 0.3 M layers (differing depending on the concentration of the ANI monomer) onto the surface of ITO to act as transporting layers that decreased the injection barrier of ITO, resulting in power conversion efficiencies of 1.33 and 1.78%, respectively. The solar cell performances—as measured by the fill factors (FF) and values of J_{SC} and V_{OC} —of the devices featuring the PANI layer were greater than that of the device featuring bare ITO. Furthermore, the power conversion efficiency of the device incorporating PANI – 0.3 M/PEDOT:PSS ($\eta=2.76\%$) was higher than those incorporating buffer layers prepared from water- and organic solvent-based PANI doped with polyacrylamide ($\eta=2.5\%$) [25], ITO/electropolymerized PEDOT:PSS ($\eta=0.33\%$) [24], a PANI layer prepared with a well-controlled electrochemical deposition time ($\eta=0.68\%$), and ITO/CNT/PEDOT:PSS ($\eta=1.74\%$) [36].

Our results indicate that the use of electrochemical deposition as well as controlling the deposition concentration of the PANI buffer layer is a promising method for the preparation of organic devices. Furthermore, we used PEDOT:PSS to cover the PANI – 0.3 M film and planarize its rough surface, thereby decreasing the probability of electrical shorts and lowering the hole injection barrier. Indeed, the PANI/PEDOT:PSS solar cell exhibited superior photovoltaic performance: a value of V_{OC} of 0.64 V, a value of J_{SC} of 7.03 mA/cm², an FF of 0.61, and a value of η of 2.76%. In contrast to the device incorporating the bare ITO anode, the values of J_{SC} and η of the solar cells increased dramatically—by 63 and 268%, respectively—for the device featuring the PANI/PEDOT:PSS-coated ITO

anode (in comparison, the corresponding device incorporating a PEDOT:PSS-coated ITO anode improved these values by only 49 and 206%, respectively). As mentioned above, the optical transmittance of the PANI/PEDOT:PSS layer was slightly lower than that of the PEDOT:PSS layer in the wavelength range 350–999,500 nm; this behavior would decrease the amount of incident light reaching the photoactive polymer. Nevertheless, the photovoltaic performance of the PANI/PEDOT:PSS solar cell was better than that of the solar cells incorporating bare ITO and PEDOT:PSS. Accordingly, we suspect that some of the excitons were swept to the well-contacted, highly ordered nano PANI/PEDOT:PSS interfacial layer under the influence of the built-in chemical and electric potentials, leading to more-efficient extraction of photoinduced holes, providing conducting pathways to the buffer layer while minimizing the degree of exciton recombination and resulting in a more-efficient charge separation. The increase in the hole transporting ability in the PANI/PEDOT:PSS layer was caused by interactions between the PANI nitrogen atoms and the functional groups of PSS, leading to additional doping of PANI (Scheme 2) and decreasing the value of R_s of the interface between the PANI film and the PEDOT:PSS buffer layer [37,38]. The enhanced hole collection can be ascribed in part to geometrical field enhancement at the PANI/PEDOT:PSS layer, similar to that observed in a previous study when PANI was used as the interlayer [24–26]. The separated free charge carriers proceeded toward their respective electrodes to generate the electric current.

4. Conclusions

We have electrochemically deposited two nano PANI buffer layers, PANI – 0.1 M and PANI – 0.3 M, as HTLs for P3HT/PCBM-based OSCs and compared their performance with those of solar cells prepared without a buffer layer (i.e., bare ITO) or with a PEDOT:PSS layer or a PANI – 0.3 M/PEDOT:PSS layer. Among these systems, the device incorporating PANI/PEDOT:PSS as the buffer layer exhibited the best photovoltaic performance: a value of V_{OC} of 0.64 V, a value of J_{SC} of 7.03 mA/cm², an FF of 0.61, and a value of η of 2.76%. The ability to transport holes in the PANI – 0.3 M/PEDOT:PSS layer increased as a result of interactions between the PANI nitrogen atoms and the functional groups of PSS, leading to additional doping of the PANI film, a decrease in the value of R_s of the interface between the PANI – 0.3 M film and the PEDOT:PSS buffer layer, and, ultimately, an increase in the power conversion efficiency. Furthermore, the combination of the electrochemical deposition of nano PANI and the spin-coating of PEDOT:PSS as the buffer layer appears to be a promising means of improving hole transport in organic-based electronics. The optimization of these devices is currently underway in our laboratory.

Acknowledgment

We thank the National Science Council of Taiwan (grant NSC-101-2221-E-151-037) for financial support.

References

- [1] J.S. Huang, P.F. Miller, J.S. Wilson, A.J. de Mello, J.C. de Mello, D.D.C. Bradley, Investigation of the effects of doping and post-deposition treatments on the conductivity, morphology, and work function of poly(3,4-ethylenedioxythiophene)/poly(styrene sulfonate) films, *Adv. Funct. Mater.* 15 (2005) 290–296.
- [2] Y.H. Kim, S.H. Lee, J. Noh, S.H. Han, Performance and stability of electro-luminescent device with self-assembled layers of poly(3,4-ethylenedioxythiophene)-poly(styrenesulfonate) and polyelectrolytes, *Thin Solid Films* 510 (2006) 305–310.
- [3] S. Rait, S. Kashyap, P.K. Bhatnagar, P.C. Mathur, S.K. Sengupta, J. Kumar, Improving power conversion efficiency in polythiophene/fullerene-based bulk heterojunction solar cells, *Sol. Energy Mater. Sol. Cells* 91 (2007) 757–763.
- [4] J. Ohshita, Y. Tada, A. Kunai, Y. Harima, A. Kohno, Y. Kunugi, Effects of annealing of poly(3-hexylthiophene) film on the performance of double-layered EL devices of ITO/polymer/Alq₃/Mg-Ag, *Synth. Met.* 157 (2007) 104–108.
- [5] Y. Yang, A.J. Heeger, Effect of substrate materials in the growth of ZnSe on GaAs and GaP substrates, *Appl. Phys. Lett.* 64 (1988) 1245–1248.
- [6] A.J. Heeger, I.D. Parker, Y. Yang, Carrier injection into semiconducting polymers: Fowler–Nordheim field-emission tunneling, *Synth. Met.* 67 (1994) 23–29.
- [7] S. Karg, J.C. Scott, J.R. Salem, M. Angelopoulos, Increased brightness and lifetime of polymer light-emitting diodes with polyaniline anodes, *Synth. Met.* 80 (1996) 111–117.
- [8] F.C. Krebs, Fabrication and processing of polymer solar cells: a review of printing and coating techniques, *Sol. Energy Mater. Sol. Cells* 93 (2009) 394–412.
- [9] K.J. Kim, Y.S. Kim, W.S. Kang, B.H. Kang, S.H. Yeom, D.E. Kim, J.H. Kim, S.W. Kang, Inspection of substrate-heated modified PEDOT:PSS morphology for all spray deposited organic photovoltaics, *Sol. Energy Mater. Sol. Cells* 94 (2010) 1303–1306.
- [10] P. Kopola, T. Aernouts, S. Guillerez, H. Jin, M. Tuomikoski, A. Maaninen, J. Hast, High efficient plastic solar cells fabricated with a high-throughput gravure printing method, *Sol. Energy Mater. Sol. Cells* 94 (2010) 1673–1680.
- [11] S.S. Kim, S.I. Na, S.J. Kang, D.Y. Kim, Annealing-free fabrication of P3HT:PCBM solar cells via simple brush painting, *Sol. Energy Mater. Sol. Cells* 94 (2010) 171–175.
- [12] F.C. Krebs, Polymer solar cell modules prepared using roll-to-roll methods: knife-over-edge coating, slot-die coating and screen printing, *Sol. Energy Mater. Sol. Cells* 93 (2009) 465–475.
- [13] B.S. Chuah, D.H. Hwang, S.T. Kim, S.C. Moratti, A.B. Holmes, J.C. deMello, R.H. Friend, New luminescent polymers for LEDs, *Synth. Met.* 91 (1997) 279–282.
- [14] R.O. Garay, B. Mayer, F.E. Karasz, R.W. Lenz, Synthesis and characterization of poly[2,5-bis(triethoxy)-1,4-phenylene vinylene], *J. Polym. Sci., Part A: Polym. Chem.* 33 (1995) 525–531.
- [15] B. Winkler, L. Dai, A.W.H. Mau, Novel poly(*p*-phenylene vinylene) derivatives with oligo(ethylene oxide) side chains: synthesis and pattern formation, *Chem. Mater.* 11 (1999) 704–711.
- [16] G. Yu, High performance photonic devices made with semiconducting polymers, *Synth. Met.* 80 (1996) 143–150.
- [17] C. Liedenbaum, Y. Croonen, P. s. J. Vleggaar, H. Schoo, Low voltage operation of large area polymer LEDs, *Synth. Met.* 91 (1997) 109–111.
- [18] H.L. Wang, A.G. MacDiarmid, Y.Z. Wang, D.D. Gebler, A.J. Epstein, Application of polyaniline (emeraldine base, EB) in polymer light-emitting devices, *Synth. Met.* 78 (1996) 33–37.
- [19] P.K.H. Ho, M. Granstrom, R.H. Friend, N.C. Greenham, Ultrathin self-assembled layers at the ITO interface to control charge injection and electroluminescence efficiency in polymer light-emitting diodes, *Adv. Mater.* 10 (1998) 769–774.
- [20] S.A. Carter, M. Angelopoulos, S. Karg, P.J. Brock, Polymeric anodes for improved polymer light-emitting diode performance, *Appl. Phys. Lett.* 70 (1997) 2067–2069.
- [21] H. Spreitzer, H. Becker, E. Kluge, W. Kreuder, H. Schenk, R. Demandt, H. Schoo, Soluble phenyl-substituted PPVs: new materials for highly efficient polymer LEDs, *Adv. Mater.* 10 (1998) 1340–1343.
- [22] J.C. Scott, S.A. Carter, S. Karg, M. Angelopoulos, Polymeric anodes for organic light-emitting diodes, *Synth. Met.* 85 (1997) 1197–1200.
- [23] J. Yan, C.H. Sun, F.U. Tan, X.J. Hu, P. Chen, S.C. Qu, S.Y. Zhou, J.K. Xu, Electropolymerized poly(3,4-ethylenedioxythiophene):poly(styrene sulfonate) (PEDOT:PSS) film on ITO glass and its application in photovoltaic device, *Sol. Energy Mater. Sol. Cells* 94 (2010) 390–394.
- [24] R. Valaski, F. Muchenski, R.M.Q. Mello, L. Micaroni, L.S. Roman, I.A. Hummelgen, Sulfonated polyaniline/poly(3-methylthiophene)-based photovoltaic devices, *J. Solid State Electrochem.* 10 (2006) 24–27.
- [25] F. Tan, S. Qu, J. Wu, Z. Wang, L. Jin, Y. Bi, J. Cao, K. Liu, J. Zhang, Z. Wang, Electrodeposited polyaniline films decorated with nano-islands: characterization and application as anode buffer layers in solar cells, *Sol. Energy Mater. Sol. Cells* 95 (2011) 440–445.
- [26] M.Y. Chang, C.S. Wu, Y.F. Chen, B.Z. Hsieh, W.Y. Huang, K.S. Ho, T.H. Hsieh, Y.K. Han, Polymer solar cells incorporating one-dimensional polyaniline nanotubes, *Org. Electron.* 9 (2008) 1136–1139.
- [27] Y.K. Kim, A.M. Ballantyne, J. Nelson, D.D.C. Bradley, Effects of thickness and thermal annealing of the PEDOT:PSS layer on the performance of polymer solar cells, *Org. Electron.* 10 (2009) 205–209.
- [28] D.J. Milliron, I.G. Hill, C. Shen, A. Kahn, J. Schwartz, Surface oxidation activates indium tin oxide for hole injection, *J. Appl. Phys.* 87 (2000) 572–576.
- [29] J.H. Choi, E.S. Lee, S.H. Choi, H.K. Baik, K.M. Song, Y.S. Lim, Work function increase of indium–tin–oxide surfaces by atmospheric air plasma treatment with steady-state airflow, *J. Vac. Sci. Technol. A* 23 (2005) 1479–1483.
- [30] W. Ma, C. Yang, X. Gong, K. Lee, A.J. Heeger, Thermally stable, efficient polymer solar cells with nanoscale control of the interpenetrating network morphology, *Adv. Funct. Mater.* 15 (2005) 1617–1622.
- [31] G. Xue, S. Uchida, B.P. Rand, S.R. Forrest, 4.2% Efficient organic photovoltaic cells with low series resistances, *Appl. Phys. Lett.* 84 (2004) 3013–3015.
- [32] F.L. Zhang, A. Gadisa, O. Inganas, M. Svensson, M.R. Andersson, Influence of buffer layers on the performance of polymer solar cells, *Appl. Phys. Lett.* 84 (2004) 3906–3908.
- [33] S. Kirchmeyer, K. Reuter, Scientific importance properties and growing applications of poly(3,4-ethylenedioxythiophene), *J. Mater. Chem.* 15 (2005) 2077–2088.
- [34] A. Elschner, F. Brudera, H.-W. Heuera, F. Jonasa, A. Karbacha, S. Kirchmeyer, S. Thurma, R. Wehrmann, PEDT/PSS for efficient hole-injection in hybrid organic light-emitting diodes, *Synth. Met.* 111–112 (2000) 139–143.
- [35] H. Bejbouji, L. Vignau, J.L. Miane, M.T. Dang, E.M. Oualim, M. Harmouchi, A. Mouhsen, Polyaniline as a hole injection layer on organic photovoltaic cells, *Sol. Energy Mater. Sol. Cells* 94 (2010) 176–181.
- [36] R. Ulbricht, S.B. Lee, X. Jiang, K. Inoue, M. Zhang, S. Fang, R.H. Baughman, A.A. Zakhidov, Transparent carbon nanotube sheets as 3-D charge collectors in organic solar cells, *Sol. Energy Mater. Sol. Cells* 91 (2007) 416–419.
- [37] O.P. Dimitriev, Cooperative doping in polyaniline-poly(ethylene-3,4-dioxythiophene):poly(styrenesulfonic acid) composite system, *J. Polym. Res.* 18 (2011) 2435–2440.
- [38] J. Kim, S. Park, N.F. Scherer, Ultrafast dynamics of polarons in conductive polyaniline: comparison of primary and secondary doped forms, *J. Phys. Chem. B* 112 (2008) 1557s6–15587.